

Combined CDF and DØ Upper Limits on Standard Model Higgs Boson Production at High Mass (155–200 GeV/c²) with 3 fb⁻¹ of data

The TEVNPH Working Group*

for the CDF and DØ Collaborations

August 30, 2021

We combine results from CDF and DØ searches for a standard model Higgs boson (H) in $p\bar{p}$ collisions at the Fermilab Tevatron at $\sqrt{s} = 1.96$ TeV. With 3.0 fb⁻¹ of data analyzed at CDF, and 3.0 fb⁻¹ at DØ, the 95% C.L. upper limits on Higgs boson production are a factor of 1.2, 1.0 and 1.3 higher than the SM cross section for a Higgs boson mass of $m_H = 165, 170$ and 175 GeV/c², respectively. We exclude at 95% C.L. a standard model Higgs boson of $m_H = 170$ GeV/c². Based on simulation, the ratios of the corresponding median expected upper limit to the Standard Model cross section are 1.2, 1.4 and 1.7. Compared to the previous Higgs Tevatron combination, more data and refined analysis techniques have been used. These results extend significantly the individual limits of each experiment and provide new knowledge on the mass of the standard model Higgs boson beyond the LEP direct searches.

Preliminary Results

* The Tevatron New-Phenomena and Higgs working group can be contacted at TEVNPHWG@fnal.gov. More information can be found at <http://tevnphwg.fnal.gov/>.

I. INTRODUCTION

The search for the last unobserved particle of the standard model (SM), the Higgs boson, has been a major goal of High Energy Physics for many years, and is a central part of Fermilab's Tevatron program. Direct searches at the CERN LEP collider have set a 95% C.L. limit on the Higgs boson mass of $m_H > 114.4$ GeV [1]. Taking into account this limit, precision electroweak measurements indirectly constrain the SM Higgs boson mass to be lower than 190 GeV at the 95% C.L. [2], which is within reach of the Fermilab Tevatron collider experiments.

Previous CDF and DØ results on Higgs searches were combined in the Tevatron Higgs combination presented in April 2008 [3]. Both CDF and DØ have recently reported new and updated searches for the SM Higgs boson [4]-[18] and their combination [19, 20].

In this note, we combine the most recent results of all such searches in $p\bar{p}$ collisions at $\sqrt{s} = 1.96$ TeV which are sensitive to a high mass (155-200 GeV/ c^2) Higgs: the searches for a SM Higgs boson decaying to WW pairs (the W 's then decaying leptonically) and produced through gluon-gluon fusion ($p\bar{p} \rightarrow H \rightarrow W^+W^-$), vector boson fusion (VBF), or in association with vector bosons ($p\bar{p} \rightarrow WH \rightarrow WW^+W^-$ and $p\bar{p} \rightarrow WH/ZH$ with hadronic W/Z decays) in data corresponding to integrated luminosities of 3.0 fb $^{-1}$ at CDF and 3.0 fb $^{-1}$ at DØ.

To simplify their combination, the searches are separated into mutually exclusive final states (see Table I and II) referred to as “analyses” in this note. Selection procedures for each analysis are detailed in Refs. [7, 8, 14, 15], and are briefly described below.

II. ACCEPTANCE, BACKGROUNDS AND LUMINOSITY

Event selections are similar for the corresponding CDF and DØ analyses. For the $H \rightarrow W^+W^-$ analyses, a large \cancel{E}_T and two opposite-signed, isolated leptons (any combination of electrons or muons) are selected, defining three final states (e^+e^- , $e^\pm\mu^\mp$, and $\mu^+\mu^-$) for DØ. CDF separates the $H \rightarrow W^+W^-$ events into five non-overlapping samples, first by separating the events by jet multiplicity (0, 1 or 2), then subdividing the 0 and 1 jet samples in two, one having a low signal/background (S/B) ratio, the other having a higher one. The presence of neutrinos in the final state prevents reconstruction of the Higgs boson mass, so other variables have to be used for separating signal from background. In these analyses, the final discriminants are neural-network outputs based on several kinematic variables [7, 14]. These include likelihoods constructed from matrix-element probabilities as input to the neural network, for CDF. All analyses in these channels have been updated with more data and analysis improvements compared to our previous combination [3].

The CDF and DØ experiments also contribute $WH \rightarrow WW^+W^-$ analyses, where the associated W boson and the W boson from the Higgs boson decay which has the same charge are required to decay leptonically, thereby defining like-sign dilepton final states ($e^\pm e^\pm$, $e^\pm\mu^\pm$, and $\mu^\pm\mu^\pm$) containing all decays of the third W boson. In these analyses, CDF derive the limits from a counting experiment, while for DØ the final variable is a likelihood discriminant formed from several topological variables.

Higgs boson signals (gluon-gluon fusion, vector boson production, or associated production with vector bosons) are simulated using PYTHIA [21], and CTEQ6L [22] parton distribution functions at leading-order (LO). The signal cross sections are normalized to next-to-next-to-leading order (NNLO) calculations [23, 24], and branching ratios from HDECAY [25]. The $gg \rightarrow H$ production cross section is also corrected for two-loop electroweak corrections [26].

For both CDF and DØ, events from multijet (instrumental) backgrounds (“QCD production”) are measured in data with different methods, in orthogonal samples. For CDF, backgrounds from other SM processes were generated using PYTHIA, ALPGEN [27], MC@NLO [28] and HERWIG [29] programs. For DØ, these backgrounds were generated using PYTHIA, ALPGEN, and COMHEP [30], with PYTHIA providing parton-showering and hadronization for all the generators. Background processes were normalized using either experimental data or next-to-leading order calculations from MCFM [31].

Integrated luminosities, and references to the Collaborations' public documentation for each analysis are given in Table I for CDF and in Table II for DØ. The tables include the ranges of Higgs boson mass (m_H) over which the searches were performed, but the combination presented in this note is performed only for search of Higgs bosons with mass of 155 GeV/ c^2 or above.

TABLE I: Luminosity, explored mass range and references for the CDF analyses. ℓ stands for either e or μ .

	$H \rightarrow W^+W^-$ 0,1 jet (low,high S/B), 2jet	$WH \rightarrow WW^+W^-$ $\rightarrow \ell^\pm \nu \ell^\pm \nu$
Luminosity (fb $^{-1}$)	3.0	1.9
m_H range (GeV/ c^2)	110-200	110-200
Reference	[7]	[8]

TABLE II: Luminosity, explored mass range and references for the DØ analyses. ℓ stands for either e or μ .

	$H \rightarrow W^+W^-$ $\rightarrow \ell^\pm \nu \ell^\mp \nu$	$WH \rightarrow WW^+W^-$ $\rightarrow \ell^\pm \nu \ell^\pm \nu$
Luminosity (fb $^{-1}$)	3.0	1.1
m_H range (GeV/ c^2)	110-200	120-200
Reference	[14]	[15]

III. COMBINING CHANNELS

To verify that the final result does not depend on the details of the statistical formulation, we performed two types of combinations, using the Bayesian and Modified Frequentist approaches, which give similar results (within 10%). Both methods rely on distributions in the final discriminants, and not just on their single integrated values. Systematic uncertainties enter as uncertainties on the expected number of signal and background events, as well as on the distribution of the discriminants in each analysis (“shape uncertainties”). Both methods use likelihood calculations based on Poisson probabilities.

A. Bayesian Method

Because there is no experimental information on the production cross section for the Higgs boson, in the Bayesian technique [19] we assign a flat prior to the total selected Higgs boson cross section. For a given Higgs boson mass, the combined likelihood is a product of likelihoods for the individual channels, each of which is a product over histogram bins:

$$\mathcal{L}(R, \vec{s}, \vec{b} | \vec{n}, \vec{\theta}) \times \pi(\vec{\theta}) = \prod_{i=1}^{N_C} \prod_{j=1}^{Nbins} \mu_{ij}^{n_{ij}} e^{-\mu_{ij}} / n_{ij}! \times \prod_{k=1}^{n_{np}} e^{-\theta_k^2/2} \quad (1)$$

where the first product is over the number of channels (N_C), and the second product is over histogram bins containing n_{ij} events, binned in ranges of the final discriminants used for individual analyses, such as the dijet mass, neural-network outputs, or matrix-element likelihoods. The parameters that contribute to the expected bin contents are $\mu_{ij} = R \times s_{ij}(\vec{\theta}) + b_{ij}(\vec{\theta})$ for the channel i and the histogram bin j , where s_{ij} and b_{ij} represent the expected background and signal in the bin, and R is a scaling factor applied to the signal to test the sensitivity level of the experiment. Truncated Gaussian priors are used for each of the nuisance parameters θ_k , which define the sensitivity of the predicted signal and background estimates to systematic uncertainties. These can take the form of uncertainties

on overall rates, as well as the shapes of the distributions used for combination. These systematic uncertainties can be far larger than the expected SM signal, and are therefore important in the calculation of limits. The truncation is applied so that no prediction of any signal or background in any bin is negative. The posterior density function is then integrated over all parameters (including correlations) except for R , and a 95% confidence level upper limit on R is estimated by calculating the value of R that corresponds to 95% of the area of the resulting distribution.

B. Modified Frequentist Method

The Modified Frequentist technique relies on the CL_s method, using a log-likelihood ratio (LLR) as test statistic:

$$LLR = -2 \ln \frac{p(\text{data}|H_1)}{p(\text{data}|H_0)}, \quad (2)$$

where H_1 denotes the test hypothesis, which admits the presence of backgrounds and a Higgs boson signal, while H_0 is the null hypothesis, for only backgrounds. The probabilities p are computed using the best-fit values of the nuisance parameters for each event, separately for each of the two hypotheses, and include the Poisson probabilities of observing the data multiplied by Gaussian constraints for the values of the nuisance parameters [32]. This technique extends the LEP procedure [33] which does not involve a fit, in order to yield better sensitivity when expected signals are small and systematic uncertainties on backgrounds are large.

The CL_s technique involves computing two p -values, CL_{s+b} and CL_b . The latter is defined by

$$1 - CL_b = p(LLR \leq LLR_{\text{obs}}|H_0), \quad (3)$$

where LLR_{obs} is the value of the test statistic computed for the data. $1 - CL_b$ is the probability of observing a signal-plus-background-like outcome without the presence of signal, i.e. the probability that an upward fluctuation of the background provides a signal-plus-background-like response as observed in data. The other p -value is defined by

$$CL_{s+b} = p(LLR \geq LLR_{\text{obs}}|H_1), \quad (4)$$

and this corresponds to the probability of a downward fluctuation of the sum of signal and background in the data. A small value of CL_{s+b} reflects inconsistency with H_1 . It is also possible to have a downward fluctuation in data even in the absence of any signal, and a small value of CL_{s+b} is possible even if the expected signal is so small that it cannot be tested with the experiment. To minimize the possibility of excluding a signal to which there is insufficient sensitivity (an outcome expected 5% of the time at the 95% C.L., for full coverage), we use the quantity $CL_s = CL_{s+b}/CL_b$. If $CL_s < 0.05$ for a particular choice of H_1 , that hypothesis is deemed excluded at the 95% C.L.

Systematic uncertainties are included by fluctuating the predictions for signal and background rates in each bin of each histogram in a correlated way when generating the pseudoexperiments used to compute CL_{s+b} and CL_b .

C. Systematic Uncertainties

Systematic uncertainties differ between experiments and analyses, and they affect the rates and shapes of the predicted signal and background in correlated ways. The combined results incorporate the sensitivity of predictions to values of nuisance parameters, and correlations are included, between rates and shapes, between signals and backgrounds, and between channels within experiments and between experiments. More on these issues can be found in the individual analysis notes [4]-[18]. Here we consider only the largest contributions and correlations between and within the two experiments.

1. Correlated Systematics between CDF and DØ

The uncertainty on the measurement of the integrated luminosity is 6% (CDF) and 6.1% (DØ). Of this value, 4% arises from the uncertainty on the inelastic $p\bar{p}$ scattering cross section, which is correlated between CDF and DØ.

The uncertainty on the production rates for the signal, for top-quark processes ($t\bar{t}$ and single top) and for electroweak processes (WW , WZ , and ZZ) are taken as correlated between the two experiments. As the methods of measuring the multijet (“QCD”) backgrounds differ between CDF and $D\bar{O}$, there is no correlation assumed between these rates. The calibrations of fake leptons and unvetoes $\gamma \rightarrow e^+e^-$ conversions, are performed by each collaboration using independent data samples and methods, hence are considered uncorrelated.

2. Correlated Systematic Uncertainties for CDF

The dominant systematic uncertainties for the CDF analyses are shown in Tables III, IV, V, and VII. Each source of uncertainty induces a correlated uncertainty across all CDF channels sensitive to that source. For $H \rightarrow W^+W^-$, the largest uncertainty comes from MC modeling (5%). For simulated backgrounds, the uncertainties on the expected rates range from 11-40% (depending on background). The backgrounds with the largest systematic uncertainties are in general quite small. Such uncertainties are constrained by fits to the nuisance parameters, and they do not affect the result significantly. Because the $H \rightarrow W^+W^-$ channel, the uncertainty on luminosity is taken to be correlated between signal and background. The differences in the resulting limits, whether treating the remaining uncertainties as correlated or uncorrelated is within 5%.

3. Correlated Systematic Uncertainties for $D\bar{O}$

The dominant systematic uncertainties for $D\bar{O}$ analyses are shown in Tables VI and VIII. Each source of uncertainty induces a correlated uncertainty across all $D\bar{O}$ channels sensitive to that source. For $H \rightarrow W^+W^-$ and $WH \rightarrow WW^+W^-$, the largest uncertainties are associated with lepton measurement and acceptance. These values range from 2-11% depending on the final state. The largest contributing factor to all analyses is the uncertainty on cross sections for simulated background, and is 6-18%. All systematic uncertainties arising from the same source are taken to be correlated between the different backgrounds and between signal and background.

TABLE III: Systematic uncertainties on the contributions for CDF's $H \rightarrow W^+W^- \rightarrow \ell^\pm \ell'^\mp$ channel with zero jets. Systematic uncertainties are listed by name, see the original references for a detailed explanation of their meaning and on how they are derived. Systematic uncertainties for $gg \rightarrow H$ shown in this table are obtained for $m_H = 160 \text{ GeV}/c^2$. Uncertainties are relative, in percent and are symmetric unless otherwise indicated. Systematic in bold are correlated across jet bins but not across channels. Systematics in italics are correlated across jet bins and across appropriate channels.

CDF: $H \rightarrow WW \rightarrow \ell^\pm \ell'^\mp + 0 \text{ Jets}$ Analysis											
Uncertainty Source	WW	WZ	ZZ	$t\bar{t}$	DY	$W\gamma$	$W+\text{jet}$	$gg \rightarrow H$	WH	ZH	VBF
Cross Section											
Scale								10.9%			
PDF Model								5.1%			
Total	<i>10.0%</i>	<i>10.0%</i>	<i>10.0%</i>	15.0%	5.0%	10.0%		12.0%			
Acceptance											
Scale (leptons)								2.5%			
Scale (jets)								4.6%			
PDF Model (leptons)	1.9%	2.7%	2.7%	2.1%	4.1%	2.2%		1.5%			
PDF Model (jets)								0.9%			
Higher-order Diagrams	5.5%	10.0%	10.0%	10.0%	5.0%	10.0%					
Missing Et Modeling	1.0%	1.0%	1.0%	1.0%	20.0%	1.0%		1.0%			
Conversion Modeling						20.0%					
Jet Fake Rates											
(Low S/B)							21.5%				
(High S/B)							27.7%				
MC Run Dependence	3.9%			4.5%		4.5%		3.7%			
Lepton ID Efficiencies	2.0%	1.7%	2.0%	2.0%	1.9%	1.4%		1.9%			
Trigger Efficiencies	2.1%	2.1%	2.1%	2.0%	3.4%	7.0%		3.3%			
Luminosity	5.9%	5.9%	5.9%	5.9%	5.9%	5.9%		5.9%			

TABLE IV: Systematic uncertainties on the contributions for CDF's $H \rightarrow W^+W^- \rightarrow \ell^\pm \ell'^\mp$ channel with one jet. Systematic uncertainties are listed by name, see the original references for a detailed explanation of their meaning and on how they are derived. Systematic uncertainties for $gg \rightarrow H$ shown in this table are obtained for $m_H = 160 \text{ GeV}/c^2$. Uncertainties are relative, in percent and are symmetric unless otherwise indicated. Negative numbers indicate systematics that are anti-correlated between channels. Systematic in bold are correlated across jet bins but not across channels. Systematics in italics are correlated across jet bins and across appropriate channels.

CDF: $H \rightarrow WW \rightarrow \ell^\pm \ell'^\mp + 1 \text{ Jet}$ Analysis											
Uncertainty Source	WW	WZ	ZZ	$t\bar{t}$	DY	$W\gamma$	W+jet	$gg \rightarrow H$	WH	ZH	VBF
Cross Section											
Scale								10.9%			
PDF Model								5.1%			
Total	10.0%	10.0%	10.0%	15.0%	5.0%	10.0%		12.0%	5.0%	5.0%	10.0%
Acceptance											
Scale (leptons)								2.8%			
Scale (jets)								-5.1%			
PDF Model (leptons)	1.9%	2.7%	2.7%	2.1%	4.1%	2.2%		1.7%	1.2%	0.9%	2.2%
PDF Model (jets)								-1.9%			
Higher-order Diagrams	5.5%	10.0%	10.0%	10.0%	5.0%	10.0%			10.0%	10.0%	10.0%
Missing Et Modeling	1.0%	1.0%	1.0%	1.0%	20.0%	1.0%		1.0%	1.0%	1.0%	1.0%
Conversion Modeling						20.0%					
Jet Fake Rates											
(Low S/B)							22.2%				
(High S/B)							31.5%				
MC Run Dependence	1.8%			2.2%		2.2%		2.6%	2.6%	1.9%	2.8%
Lepton ID Efficiencies	2.0%	2.0%	2.2%	1.8%	2.0%	2.0%		1.9%	1.9%	1.9%	1.9%
Trigger Efficiencies	2.1%	2.1%	2.1%	2.0%	3.4%	7.0%		3.3%	2.1%	2.1%	3.3%
Luminosity	5.9%	5.9%	5.9%	5.9%	5.9%	5.9%		5.9%	5.9%	5.9%	5.9%

TABLE V: Systematic uncertainties on the contributions for CDF's $H \rightarrow W^+W^- \rightarrow \ell^\pm \ell'^\mp$ channel with two or more jets. Systematic uncertainties are listed by name, see the original references for a detailed explanation of their meaning and on how they are derived. Systematic uncertainties for $gg \rightarrow H$ shown in this table are obtained for $m_H = 160 \text{ GeV}/c^2$. Uncertainties are relative, in percent and are symmetric unless otherwise indicated. Systematic in bold are correlated across jet bins but not across channels. Systematics in italics are correlated across jet bins and across appropriate channels.

CDF: $H \rightarrow WW \rightarrow \ell^\pm \ell'^\mp + \geq 2$ Jets Analysis											
Uncertainty Source	WW	WZ	ZZ	$t\bar{t}$	DY	$W\gamma$	$W+\text{jet}$	$gg \rightarrow H$	WH	ZH	VBF
Cross Section											
Scale								10.9%			
PDF Model								5.1%			
Total	<i>10.0%</i>	<i>10.0%</i>	<i>10.0%</i>	15.0%	5.0%	10.0%		12.0%	5.0%	5.0%	10.0%
Acceptance											
Scale (leptons)								3.1%			
Scale (jets)								-8.7%			
PDF Model (leptons)	1.9%	2.7%	2.7%	2.1%	4.1%	2.2%		2.0%	1.2%	0.9%	2.2%
PDF Model (jets)								-2.8%			
Higher-order Diagrams	10.0%	10.0%	10.0%	10.0%	10.0%	10.0%			<i>10.0%</i>	<i>10.0%</i>	<i>10.0%</i>
Missing Et Modeling	1.0%	1.0%	1.0%	1.0%	20.0%	1.0%		1.0%	1.0%	1.0%	1.0%
Conversion Modeling						20.0%					
b -tag Veto				7.0%							
Jet Fake Rates							27.1%				
MC Run Dependence	1.0%			1.0%		1.0%		1.7%	2.0%	1.9%	2.6%
Lepton ID Efficiencies	1.9%	2.9%	1.9%	1.9%	1.9%	1.9%		1.9%	1.9%	1.9%	1.9%
Trigger Efficiencies	2.1%	2.1%	2.1%	2.0%	3.4%	7.0%		3.3%	2.1%	2.1%	3.3%
Luminosity	5.9%	5.9%	5.9%	5.9%	5.9%	5.9%		5.9%	5.9%	5.9%	5.9%

TABLE VI: Systematic uncertainties on the contributions for DØ's $H \rightarrow WW \rightarrow \ell^\pm \ell'^\mp$ channel. Systematic uncertainties are listed by name, see the original references for a detailed explanation of their meaning and on how they are derived. Systematic uncertainties shown in this table are obtained for the $m_H = 160 \text{ GeV}/c^2$ Higgs selection. Uncertainties are relative, in percent.

DØ: $H \rightarrow WW \rightarrow \ell^\pm \ell'^\mp$ Analysis										
	Σ Bkgd	Signal	$Z \rightarrow \ell\ell$	$Z \rightarrow \tau\tau$	$W + jets/\gamma$	$t\bar{t}$	ZZ	WZ	WW	QCD
Jet energy scale	7	3	7	6	6	7	2	1	1	-
Jet energy resol.	3	3	3	4	4	3	3	3	2	-
Jet ID	4	0	5	13	6	2	1	4	0	-
\mathcal{L} Reweighting	0	3	0	13	3	1	0	0	0	-
Beam Reweighting	2	1	2	6	4	1	1	2	1	-
$Z - p_T$ Rew	13	0	17	14	0	0	0	0	0	-
Lepton momentum	4	0	5	4	3	2	1	2	0	-
Cross section	-	10	6	6	20	10	6	6	6	-
<i>QCD</i>	-	-	-	-	-	-	-	-	-	30
Normalization	7	7	-	-	-	-	-	-	-	-
Lepton ID	4	4	-	-	-	-	-	-	-	-

TABLE VII: Systematic uncertainties on the contributions for CDF 's $WH \rightarrow WWW \rightarrow \ell'^{\pm}\ell'^{\pm}$ channel. Systematic uncertainties are listed by name, see the original references for a detailed explanation of their meaning and on how they are derived. Systematic uncertainties for WH shown in this table are obtained for $m_H = 160 \text{ GeV}/c^2$. The diboson contribution to the final selected sample is negligible. Uncertainties are relative, in percent.

CDF : $WH \rightarrow WWW \rightarrow \ell'^{\pm}\ell'^{\pm}$ Analysis.

Contribution	γ Conversions	Fakes	WH
Statistical Uncertainty	0	0	1.6
Fake Rate	0	25	0
Conversions	25	0	0
Luminosity	0	0	6
ISR	0	0	4.0
FSR	0	0	4.1
PDF	0	0	1.9
Lepton ID	0	0	1.2

TABLE VIII: Systematic uncertainties on the contributions for DØ's $WH \rightarrow WWW \rightarrow \ell'^{\pm}\ell'^{\pm}$ channel. Systematic uncertainties are listed by name, see the original references for a detailed explanation of their meaning and on how they are derived. Systematic uncertainties for WH shown in this table are obtained for $m_H = 160 \text{ GeV}/c^2$. Uncertainties are relative, in percent and are symmetric unless otherwise indicated.

DØ: $WH \rightarrow WWW \rightarrow \ell'^{\pm}\ell'^{\pm}$ Analysis.

Contribution	WZ/ZZ	Charge flips	QCD	WH
Trigger eff.	5	0	0	5
Lepton ID/Reco. eff	10	0	0	10
Cross Section	7	0	0	6
Normalization	6	0	0	0
Instrumental-ee (ee final state)	0	32	15	0
Instrumental-em ($e\mu$ final state)	0	0	18	0
Instrumental-mm ($\mu\mu$ final state)	0	$^{+290}_{-100}$	32	0

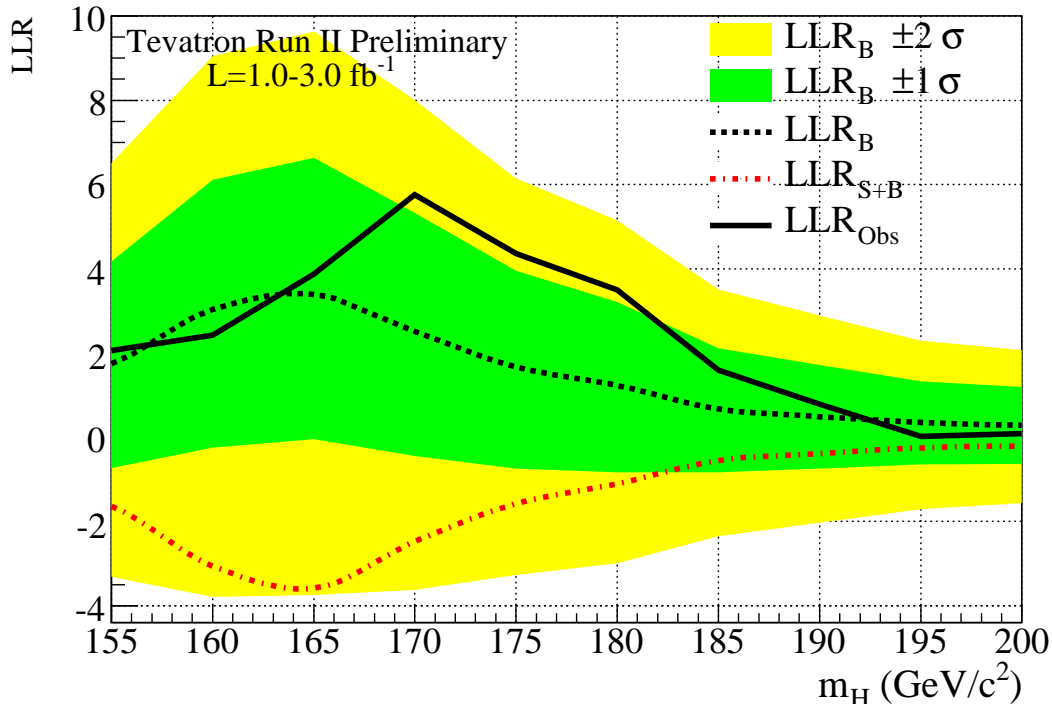


FIG. 1: Distributions of LLR as a function of the Higgs boson mass (in steps of 5 GeV/c^2) for the combination of the CDF and DØ analyses.

IV. COMBINED RESULTS

Before extracting the combined limits we study the distributions of the log-likelihood ratio (LLR) for different hypotheses, to check the expected sensitivity across the mass range tested. Figure 1 displays the LLR distributions for the combined analyses as a function of m_H . Included are the results for the background-only hypothesis (LLR_b), the signal and background hypothesis (LLR_{s+b}), and for the data (LLR_{obs}). The shaded bands represent the 1 and 2 standard deviation (σ) departures for LLR_b .

These distributions can be interpreted as follows: The separation between LLR_b and LLR_{s+b} provides a measure of the discriminating power of the search; the size of the 1- and 2- σ LLR_b bands provides an estimate of how sensitive the analysis is to a signal-plus-background-like fluctuation in data, taking account of the systematic uncertainties; the value of LLR_{obs} relative to LLR_{s+b} and LLR_b indicates whether the data distribution appears to be more signal-plus-background-like (i.e. closer to the LLR_{s+b} distribution, which is negative by construction) or background-like; the significance of any departures of LLR_{obs} from LLR_b can be evaluated by the width of the LLR_b bands.

Using the combination procedures outlined in Section III, we extract limits on SM Higgs boson production $\sigma \times B(H \rightarrow X)$ in $p\bar{p}$ collisions at $\sqrt{s} = 1.96$ TeV for $m_H = 155 - 200$ GeV/c^2 . To facilitate comparisons with the standard model and to accommodate analyses with different degrees of sensitivity, we present our results in terms of the ratio of obtained limits to cross section in the SM, as a function of Higgs boson mass, for test masses for which both experiments have performed dedicated searches in different channels. A value of the combined limit ratio which

is less or equal to one would indicate that that particular Higgs boson mass is excluded at the 95% C.L.

The combinations of results of each single experiment, yield the following ratios of 95% C.L. observed (expected) limits to the SM cross section: 1.6 (1.6) for CDF and 2.0 (1.9) for DØ at $m_H = 165 \text{ GeV}/c^2$, and 1.8 (1.9) for CDF and 1.7 (2.3) for DØ at $m_H = 170 \text{ GeV}/c^2$.

The ratios of the 95% C.L. expected and observed limit to the SM cross section are shown in Figure 2 for the combined CDF and DØ analyses. The observed and median expected ratios are listed for the tested Higgs boson masses in Tables IX and X, with observed (expected) values of 1.2 (1.2) at $m_H = 165 \text{ GeV}/c^2$, 1.0 (1.4) at $m_H = 170 \text{ GeV}/c^2$, and 1.3 (1.7) at $m_H = 175 \text{ GeV}/c^2$. We exclude at the 95% C.L. the production of a standard model Higgs boson with mass of $170 \text{ GeV}/c^2$. This result is obtained with both Bayesian and CL_S calculations.

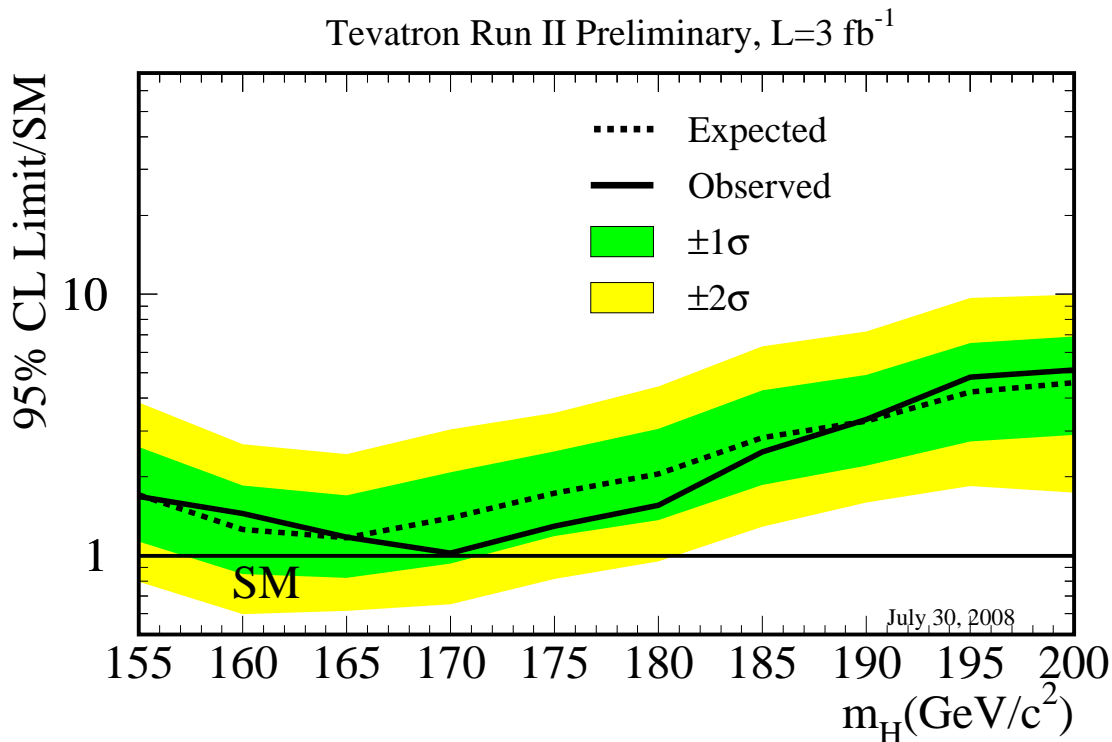


FIG. 2: Observed and expected (median, for the background-only hypothesis) 95% C.L. upper limits on the ratios to the SM cross section, as functions of the Higgs boson mass for the combined CDF and DØ analyses. The limits are expressed as a multiple of the SM prediction for test masses (every $5 \text{ GeV}/c^2$) for which both experiments have performed dedicated searches in different channels. The points are joined by straight lines for better readability. The bands indicate the 68% and 95% probability regions where the limits can fluctuate, in the absence of signal. The limits displayed in this figure are obtained with the Bayesian calculation.

We also show in Figure 3 the $1-CL_S$ distribution as a function of the Higgs boson mass, which is directly interpreted as the level of exclusion of our search. For instance, both our observed and expected results exclude a Higgs boson with $m_H = 165 \text{ GeV}/c^2$ at $\approx 92\%$ C.L.

TABLE IX: Ratios of median expected and observed 95% CL limit to the SM cross section for the combined CDF and DØ analyses as a function of the Higgs boson mass in GeV/c^2 , obtained with the Bayesian method.

	155	160	165	170	175	180	185	190	195	200
Expected	1.7	1.3	1.2	1.4	1.7	2.0	2.8	3.3	4.2	4.6
Observed	1.7	1.4	1.2	1.0	1.3	1.6	2.5	3.3	4.8	5.1

TABLE X: Ratios of median expected and observed 95% CL limit to the SM cross section for the combined CDF and DØ analyses as a function of the Higgs boson mass in GeV/c^2 , obtained with the CL_S method.

	155	160	165	170	175	180	185	190	195	200
Expected	1.6	1.2	1.1	1.3	1.7	2.0	2.8	3.4	4.2	4.7
Observed	1.6	1.3	1.1	0.95	1.2	1.4	2.3	3.2	4.7	5.0

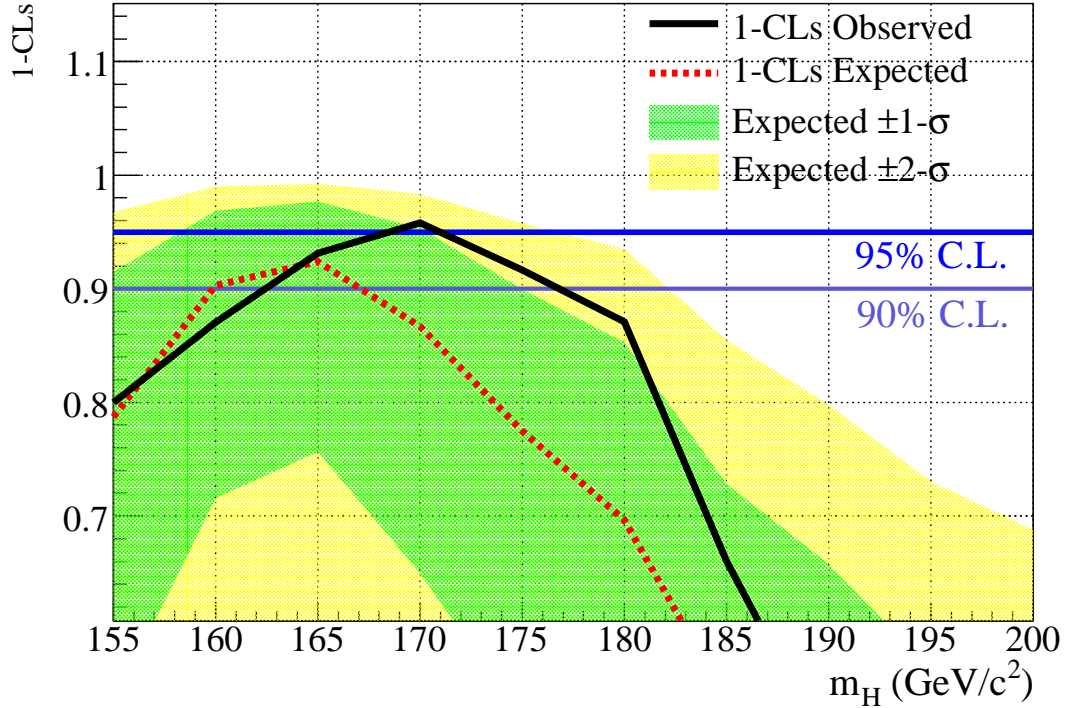


FIG. 3: Distributions of $1-CL_S$ as a function of the Higgs boson mass (in steps of $5 \text{ GeV}/c^2$) for the combination of the CDF and DØ analyses.

-
- [1] ALEPH, DELPHI, L3, and OPAL Collaborations, The LEP Working Group for Higgs Boson Searches, Phys. Lett. B **565**, 61 (2003).
 - [2] LEP Electroweak Working Group,
<http://lepewwg.web.cern.ch/LEPEWWG/>
 - [3] CDF and DØ Collaborations, “Combined CDF and DØ Upper Limits on Standard Model Higgs-Boson Production with up to 2.4 fb⁻¹ of data”, FERMILAB-PUB-08-069-E, [arXiv:0804.3423].
 - [4] CDF Collaboration, “Search for Higgs Boson Production in Association with W Boson with 2.7 fb⁻¹”, CDF Conference Note, <http://www-cdf.fnal.gov/physics/new/hdg/hdg.html>
 - [5] CDF Collaboration, “Search for the Standard Model Higgs Boson in the Missing Et and B-jets Signature”, CDF Conference Note, <http://www-cdf.fnal.gov/physics/new/hdg/hdg.html>
 - [6] CDF Collaboration, “Search for ZH in 2.4 fb⁻¹”, CDF Conference Note, <http://www-cdf.fnal.gov/physics/new/hdg/hdg.html>
 - [7] CDF Collaboration, “Search for $H \rightarrow WW$ Production Using 3.0 fb⁻¹”, CDF Conference Note, <http://www-cdf.fnal.gov/physics/new/hdg/hdg.html>
 - [8] CDF Collaboration, “Search for WH Production Using High- p_T Isolated Like-Sign Dilepton Events in Run II with 1.9 fb⁻¹”. CDF Conference Note 7307.
 - [9] CDF Collaboration, “Search for SM Higgs using tau leptons using 2 fb⁻¹”, CDF Conference Note 9179.
 - [10] DØ Collaboration, “A Search for Associated W and Higgs Production in $p\bar{p}$ Collisions at $\sqrt{s} = 1.96$ TeV”, to be submitted to Phys. Rev. Lett.
 - [11] DØ Collaboration, “Search for WH Production at $\sqrt{s} = 1.96$ TeV with Neural Networks,” DØ Conference Note 5472.
 - [12] DØ Collaboration, “Search for the standard model Higgs boson in the $HZ \rightarrow b\bar{b}\nu\nu$ channel in 2.1 fb⁻¹ of ppbar collisions at $\sqrt{s} = 1.96$ TeV”, DØ Conference note 5586.
 - [13] DØ Collaboration, “A Search for $ZH \rightarrow \ell^+\ell^-\bar{b}b$ Production at DØ in $p\bar{p}$ Collisions at $\sqrt{s} = 1.96$ TeV”, DØ Conference Note 5570.
 - [14] DØ Collaboration, “Search for the Higgs boson in $H \rightarrow WW^*$ decays with 3.0 fb⁻¹ at DØ in Run II”, DØ Conference Note 5757.
 - [15] DØ Collaboration, “Search for associated Higgs boson production $WH \rightarrow WWW^* \rightarrow \ell^\pm\nu\ell'^\pm\nu' + X$ in $p\bar{p}$ collisions at $\sqrt{s} = 1.96$ TeV”, DØ Conference Note 5485.
 - [16] DØ Collaboration, “Search for the standard model Higgs boson in $t\bar{t}$ Higgs production, DØ Conference Note 5739.
 - [17] DØ Collaboration, “Search for the Standard Model Higgs Boson in the WH to $\tau\nu b\bar{b}$ channel” DØ Conference Note 5669.
 - [18] DØ Collaboration, “Search for a light Higgs boson in $\gamma\gamma$ final state”, DØ Conference Note 5737.
 - [19] CDF Collaboration, “Combined Upper Limit on Standard Model Higgs Boson Production”, CDF Conference Note, <http://www-cdf.fnal.gov/physics/new/hdg/hdg.html>
 - [20] DØ Collaboration, “Combined upper limits on standard model Higgs boson production from the D0 experiment with 1.1-2.4 fb⁻¹” DØ Conference Note 5756.
 - [21] T. Sjostrand, L. Lonnblad and S. Mrenna, “PYTHIA 6.2: Physics and manual,” [arXiv:hep-ph/0108264].
 - [22] H. L. Lai *et al.*, “Improved Parton Distributions from Global Analysis of Recent Deep Inelastic Scattering and Inclusive Jet Data”, Phys. Rev D **55**, 1280 (1997).
 - [23] S. Catani, D. de Florian, M. Grazzini and P. Nason, “Soft-gluon resummation for Higgs boson production at hadron colliders,” JHEP **0307**, 028 (2003) [arXiv:hep-ph/0306211].
 - [24] K. A. Assamagan *et al.* [Higgs Working Group Collaboration], “The Higgs working group: Summary report 2003,” [arXiv:hep-ph/0406152].
 - [25] A. Djouadi, J. Kalinowski and M. Spira, “HDECAY: A program for Higgs boson decays in the standard model and its supersymmetric extension,” Comput. Phys. Commun. **108**, 56 (1998) [arXiv:hep-ph/9704448].
 - [26] U. Aglietti, R. Bonciani, G. Degraasi and A. Vicini, [arXiv:hep-ph/0610033].
 - [27] M. L. Mangano, M. Moretti, F. Piccinini, R. Pittau and A. D. Polosa, “ALPGEN, a generator for hard multiparton processes in hadronic collisions,” JHEP **0307**, 001 (2003) [arXiv:hep-ph/0206293].
 - [28] S. Frixione and B.R. Webber, JHEP **06**, 029 (2002) [arXiv:hep-ph/0204244].
 - [29] G. Corcella *et al.*, “HERWIG 6: An event generator for hadron emission reactions with interfering gluons (including supersymmetric processes),” JHEP **0101**, 010 (2001) [arXiv:hep-ph/0011363].
 - [30] A. Pukhov *et al.*, “CompHEP: A package for evaluation of Feynman diagrams and integration over multi-particle phase space. User’s manual for version 33,” [arXiv:hep-ph/9908288].
 - [31] J. Campbell and R. K. Ellis, <http://mcfm.fnal.gov/>.
 - [32] W. Fisher, “Systematics and Limit Calculations,” FERMILAB-TM-2386-E.

- [33] T. Junk, Nucl. Instrum. Meth. A434, p. 435-443, 1999, A.L. Read, "Modified frequentist analysis of search results (the CL_s method)", in F. James, L. Lyons and Y. Perrin (eds.), *Workshop on Confidence Limits*, CERN, Yellow Report 2000-005, available through `cdsweb.cern.ch`.